Electrical Engineering (2019) 101:969–982
https://doi.org/10.1007/s00202-019-00833-6

ORIGINAL PAPER

Optimized tuning of power oscillation damping controllers using probabilistic approach to enhance small-signal stability considering stochastic time delay

Samundra Gurung[1] · Francisco Jurado[2] · Sumate Naetiladdanon[1] · Anawach Sangswang[1]

Received: 1 April 2019 / Accepted: 9 September 2019 / Published online: 23 September 2019

Abstract
Communication latency which inherently occurs in wide area measurement system greatly degrades small-signal stability (SSS) and is stochastic in nature, and thus, the current power oscillation damping controllers (PODCs) designed to improve SSS must consider this crucial factor. This paper proposes a probabilistic method to tune the parameters of PODCs incorporated in renewable farms to improve SSS under stochastic time delay and under other power system uncertainties arising due to renewable energy resources and loads. The proposed method is composed of two stages: The first stage quantifies the effect of time delay and other power system uncertainties on SSS, and the second stage uses this information to formulate an optimization problem. This optimization problem is solved with the help of four swarm intelligence-based optimization algorithms which are: bat algorithm, cuckoo search algorithm, firefly algorithm, and particle swarm optimization algorithm. The solutions from all these four optimization algorithms are compared, and the best result is used to optimize the parameters of the PODCs. All the analyses were conducted on a modified IEEE 68 bus system. The results show that the PODCs tuned using the proposed method greatly enhances the SSS margin under different scenarios and are probabilistically robust to the varying time delay and other power system uncertainties.

Keywords Cumulant · Probability function · Swarm intelligence algorithms · Wide area damping controller

1 Introduction

1.1 Problem statement

The wide area measurement system (WAMS) utilizes the phasor measurement unit (PMU) to measure different electrical variables and a communication channel to transmit this information to the control system. The signals from WAMS have a high observability of inter-area modes which can then serve as feedback for different power system damping controllers to greatly enhance small-signal stability (SSS) of the power system [1]. However, WAMS suffers from communication delay whose value depends on the communication link used and can severely degrade SSS [1].

Besides communication latency, there are several other power system parameters which have a detrimental effect on SSS. Among them, the two main uncertain parameters affecting SSS are renewable energy resources (RES) and varying loads [2]. RES have a fluctuating output which generally has an adverse effect on SSS [3–6]. The uncertainty in load can be due to several factors such as economic and demographic factors and daily and seasonal load cycles and is also considered as a high-risk factor for low-frequency oscillatory instability [7].

✉ Francisco Jurado
fjurado@ujaen.es

Samundra Gurung
samundra24@gmail.com

Sumate Naetiladdanon
sumate.nae@kmutt.ac.th

Anawach Sangswang
anawach.san@kmutt.ac.th

[1] Department of Electrical Engineering, King Mongkut's University of Technology Thonburi, Bangkok 10140, Thailand

[2] Department of Electrical Engineering, EPS Linares, University of Jaen, 23700 Jaén, Spain

1.2 Literature review

There are many studies which have designed power oscillation damping controllers (PODC) to nullify the effect of the time delay in WAMS and improve SSS. PODCs can be conveniently integrated with different power system actuators such as flexible ac transmission system (FACTS) [1, 8], RES converter [9–12], high-voltage DC controller (HVDC) [13, 14], and battery energy storage systems (BESS) [15, 16]. The design of PODC is generally done using four methods: residue method [13, 17], robust control method [1, 12], optimization-based method [10, 18], and adaptive method [19, 20]. Most of these researches [1, 13, 16, 17] provide in-depth analysis and the controllers so designed show good performance for oscillation damping but were only done considering fixed time delay. However, the real-world time delay in WAMS is stochastic in nature [21] and the controllers designed for fixed time delay may not perform satisfactorily when the variable delay is considered [12]. There are different researches [12, 18–20, 22, 23] which have considered this crucial factor and the controllers designed by taking this consideration is highly successful in enhancing SSS compared to controllers considering only the fixed time delay model. However, the time delay is only one important uncertain parameter in the power system and the PODCs so designed taking only this variable into consideration may not be able to greatly enhance SSS when other uncertainties are also considered and should be investigated.

Probabilistic methods are well equipped to analyze uncertainties due to its mathematical nature and are found to be more efficient and robust than controllers designed using deterministic methods [14, 24]. A probabilistic method based on combination of analytical method and differential evolution algorithm is used to tune power system stabilizers (PSSs) considering generation and load uncertainty in [25]. The researchers of [9] have investigated the coordinated use of wind turbine generation (WTG) with PODCs considering stochastic wind output power and load uncertainty and observed that their proposed strategy provides good performance against these uncertainties. The researchers of [8] have coordinated static var compensator (SVC) with PSSs to improve probabilistic small-signal stability (PSSS) using the fruit-fly algorithm. A design method to tune PSSs based on the expectation model considering stochastic time delay is used in [26] and the researchers have shown that the designed PSSs can successfully nullify the effect of variable time delay and simultaneously improve SSS. An efficient probabilistic model of WTG is proposed in [24], and the authors have shown that the PSSs tuned using their developed probabilistic method outperforms deterministic method such as H-infinity control. All of these researches show the effectiveness of the probabilistic method to improve PSSS considering different kinds of uncertainties. However, most of them have not considered the effect of variable time delay [8, 9, 14, 24, 25] or has not considered the effect of other crucial power system uncertainties [26]. This paper proposes a method based on a probabilistic approach to optimize the parameters of PODCs which are assumed to be incorporated in RES converters to improve PSSS considering different power system uncertainties. The proposed method is a combination of two stages: the first stage which models the uncertain power system parameters (RES, load and time delay) and quantifies their effect on PSSS. The second stage utilizes this statistical information to coordinate the PODCs. This coordination is achieved by formulating the problem of coordination as an optimization problem which is solved using four swarm intelligence-based optimization algorithms (SIOA). Finally, the best result among the four SIOAs is used to set the parameters of PODCs. Thus, the major contributions of this paper are:

i. Development of a novel method based on probabilistic approach to optimize the PODCs incorporated in RES to improve SSS considering different critical power system uncertainties.
ii. The proposed method uses different popular SIOA such as firefly algorithm, bat algorithm, cuckoo search algorithm, and particle swarm optimization to optimize the PODC parameters. Thus, this paper also conducts comparative analysis of different SIOA.

1.3 Paper organization

The paper is structured as follows: Section 2 provides a brief overview of the proposed method, and Sect. 3 discusses the procedure to obtain the statistical information about SSS, followed by the design and optimization of PODCs in Sect. 4. Section 5 discusses the results obtained, and the conclusions drawn are provided in Sect. 6.

2 Proposed method

2.1 Overview of the power system with PODCs

A general diagram showing the utilization of WAMS to damp power system oscillation through RES converters is shown in Fig. 1. We have considered WTG and photovoltaic generation (PVG) as the two RES in our study as they are the two current leading choices of variable generation to produce electricity [27]. The PMU samples the electrical variables and sends the signal to control stations of wind and solar farm through some communication link. The computer of the control station which functions as a PODC utilizes

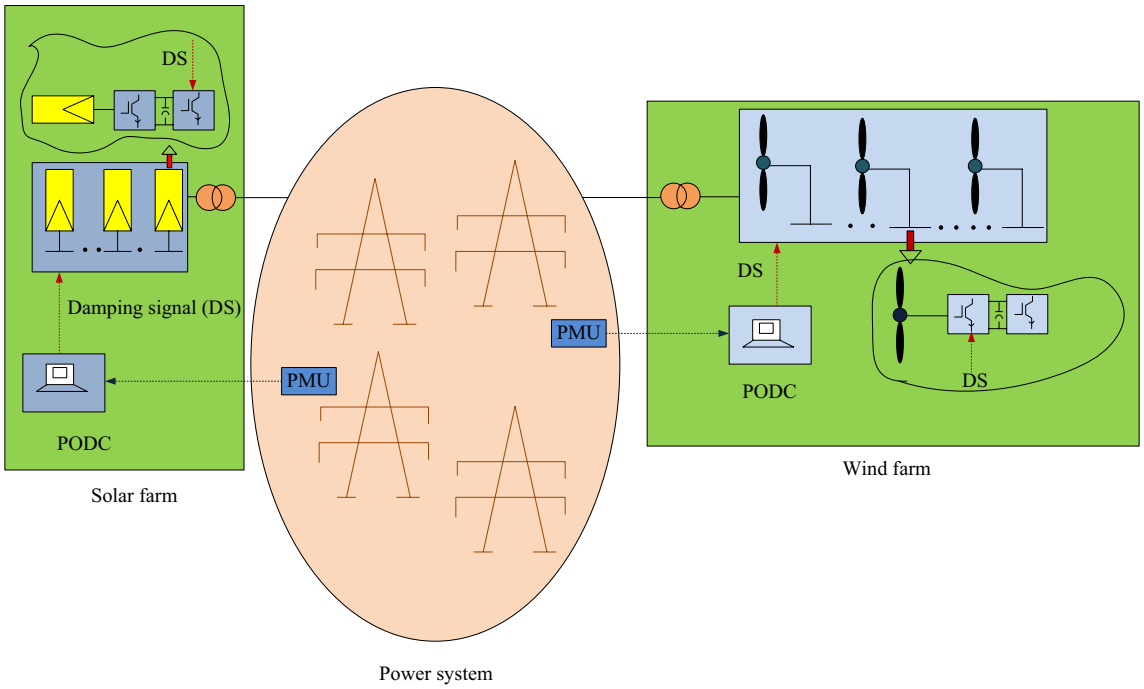

Fig. 1 Pictorial description of the usage of WAMS for power system oscillation damping

this signal from WAMS to synthesize the damping signal which is then send to the RES converter to enhance SSS.

2.2 Overview of the application of proposed method to optimize PODC parameters

Our study mainly focuses on the procedure to tune the PODCs of renewable farms to improve PSSS considering different power system uncertainties. The block diagram depicting the proposed method to tune the PODCs is shown in Fig. 2. The procedure to tune the PODCs using the proposed method is as follows:

i. Define the probabilistic model of different power system uncertainties such as time delay, RES and load, which is described in detail in Sect. 3.1.

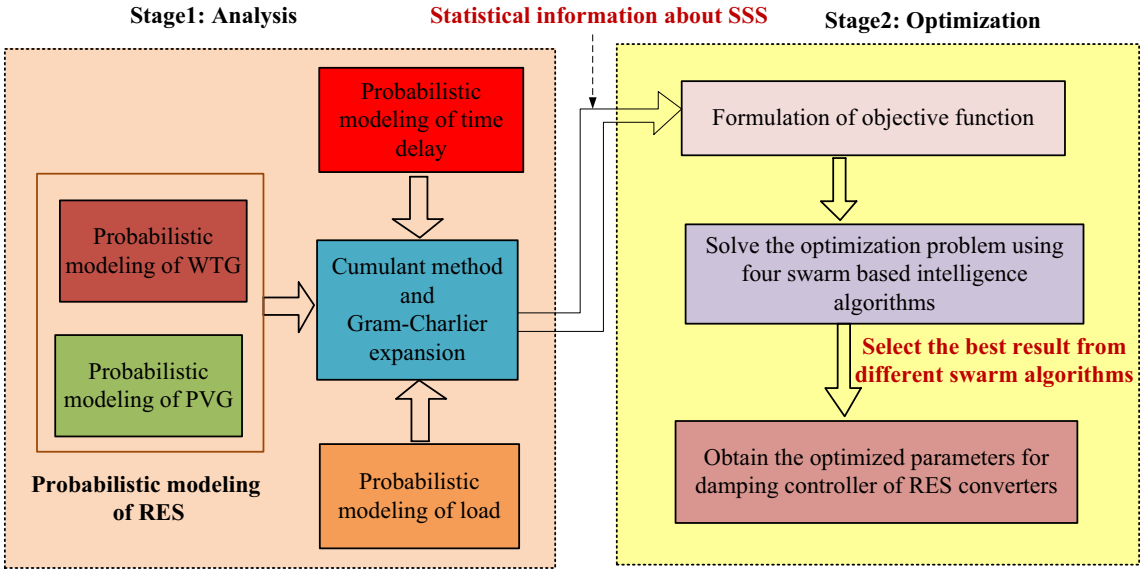

Fig. 2 Proposed method to tune the PODCs under power system uncertainties

ii. Once the input uncertainties are probabilistically modeled, the combined method of cumulant and Gram–Charlier expansion [28] is used to obtain vital statistical information about the SSS. The cumulant method is so chosen compared to other analytical methods such as point estimate and probabilistic collocation due to its higher accuracy [28]. This step is described in Sect. 3.2.
iii. The statistical information from the previous step is then used to formulate an objective function and the problem of tuning the parameters of PODCs is treated as an optimization problem whose details can be found in Sect. 4.2.1.
iv. The optimization problem is solved using meta-heuristic optimization algorithms. We have used four popular and well-established SIOAs in our study: bat algorithm (BA), cuckoo search algorithm (CSA), firefly algorithm (FA), and particle swarm optimization (PSO), and the result from the best-performing algorithm among them is finally used to tune the PODC parameters. More explanations of this step are given in Sect. 4.2.2.

3 Analysis of PSSS considering stochastic time delay and other power system uncertainties

Broadly speaking, the problem of PSSS assessment can be described as a functional relationship of output random variables (damping constant and damping factor of eigenvalue for our study) with the input random variables and can be described as:

$$\begin{aligned} \alpha_k &= f\left(P_{i,\text{res}}, P_{i,l}, T_{i,d}\right) \\ \xi_k &= f\left(P_{i,\text{res}}, P_{i,l}, T_{i,d}\right) \end{aligned} \tag{1}$$

where α_k is the damping constant for kth eigenvalue, ξ_k is the damping factor for kth eigenvalue, $P_{i,\text{res}}$ is the probability density function (PDF) of the output power of ith RES, $P_{i,l}$ is the PDF of output power of ith load, and $T_{i,d}$ is the PDF of time delay for ith PODC controller. This section discusses the procedure to model the input uncertainties and uses it with an analytical method to obtain the statistical information about the output random variables.

3.1 PDF of power system uncertainties

3.1.1 The probabilistic model of time delay

The value of latency in WAMS greatly depends on different factors such as the location of PMU units, communication link, the reliability of the communication link [29] and is thus stochastic in nature [21]. This paper model the time delay in WAMS as a normal distribution [30, 31], but other distribution can also be used if the historical data are available. Thus, the PDF of time delay for ith PODC can be written as:

$$f\left(T_{i,d}\right) = \frac{1}{\sigma_{T_{i,d}}\sqrt{2\pi}} \exp - \frac{\left(T_{i,d} - \mu_{T_{i,d}}\right)^2}{2\sigma_{T_{i,d}}^2} \tag{2}$$

where $\mu_{T_{i,d}}$ and $\sigma_{T_{i,d}}$ are the mean and standard deviation of time delay for ith PODC, respectively. Figure 3 shows the probability density of time delay used throughout in our study and the values of $\mu_{T_{i,d}}$, and $\sigma_{T_{i,d}}$ taken to construct this plot are 0.5 s, and 25%, respectively. These values ensure that the PDF of time delay covers the range of real-world WAMS delay which varies from 0.1 to 0.7 s [29].

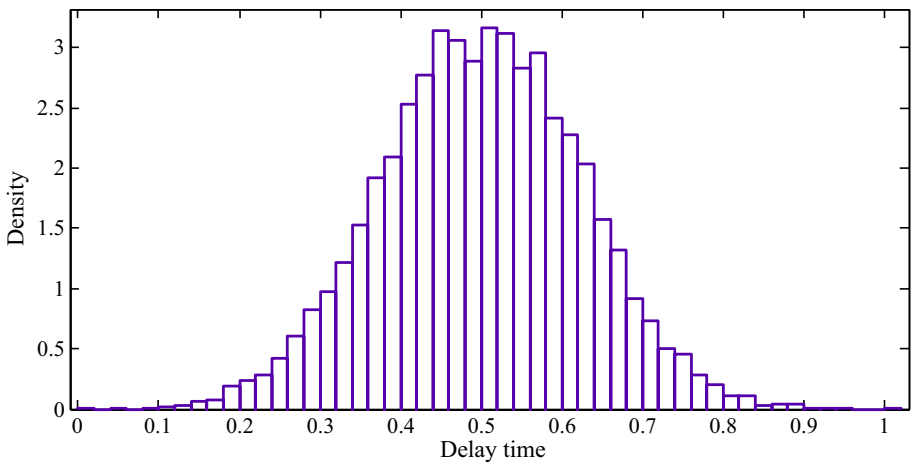

Fig. 3 Probabilistic model of time delay

3.1.2 The probabilistic model of RES

As stated earlier, our study considers two main RES: PVG and WTG. Thus, the PDF of RES $P_{i,\text{res}} = [P_{i,\text{pvg}}, P_{i,\text{wtg}}]$ where $P_{i,\text{pvg}}, P_{i,\text{wtg}}$ are the PDF of output power for ith PVG and WTG, respectively. The PDF of the output power of both PVG and WTG can be modeled as a normal distribution [10].

The PDF of the output power of ith solar farm can be computed as:

$$f\left(P_{i,\text{pvg}}\right) = \frac{1}{\sigma_{P_{i,\text{pv}}}\sqrt{2\pi}}\exp - \frac{\left[P_{i,\text{pvg}} - \left(\bar{P}_{i,\text{pvg}} + \mu_{P_{i,\text{pvg}}}\right)\right]^2}{2\sigma^2_{P_{i,\text{pvg}}}} \tag{3}$$

where $\mu_{P_{i,\text{pvg}}}, \sigma_{P_{i,\text{pvg}}}, \bar{P}_{i,\text{pvg}}$ are the mean and standard deviation of solar power forecast error, and forecast output power for ith solar farm, respectively.

The PDF of the output power of ith wind farm can be computed as:

$$f\left(P_{i,\text{wtg}}\right) = \frac{1}{\sigma_{P_{i,\text{wtg}}}\sqrt{2\pi}}\exp - \frac{\left[P_{i,\text{wtg}} - \left(\bar{P}_{i,\text{wtg}} + \mu_{P_{i,\text{wtg}}}\right)\right]^2}{2\sigma^2_{P_{i,\text{wtg}}}} \tag{4}$$

where $\mu_{P_{i,\text{wtg}}}, \sigma_{P_{i,\text{wtg}}}$, and $\bar{P}_{i,\text{wtg}}$ are the mean, standard deviation of wind power forecast error, and forecast output power for ith wind farm, respectively.

3.1.3 The probabilistic model of load

The power system loads are also commonly modeled as a normal distribution [7] and thus, the PDF of the output power of load at ith location is given by:

$$f\left(P_{i,l}\right) = \frac{1}{\sigma_{P_{i,l}}\sqrt{2\pi}}\exp - \frac{\left[P_{i,l} - \mu_{P_{i,l}}\right]^2}{2\sigma^2_{P_{i,l}}} \tag{5}$$

where $\mu_{P_{i,l}}, \sigma_{P_{i,l}}$ are the mean and standard deviation of ith load, respectively.

3.2 Calculation of stability indices

Let $\lambda_k = \alpha_k + j\omega_k$ be the kth eigenvalue, where α_k and ω_k are the damping constant and damping factor of kth eigenvalue, respectively. The damping factor ξ_k for kth eigenvalue can be calculated as [32]:

$$\xi_k = \frac{-\alpha_k}{\sqrt{\alpha_k^2 + \omega_k^2}} \tag{6}$$

Once the input uncertainties are modeled given by Eqs. (2), (3), (4), (5), the combined method of cumulant and Gram–Charlier expansion method [3–5] is used to calculate the following probabilistic stability indices in our study:

$$P(\alpha_k < \alpha_c) = \int_{-\infty}^{\alpha_c} \Phi\left(\alpha_c\right) + \frac{c_1(\alpha)}{1!}\Phi^{(1)}\left(\alpha_c\right) + \frac{c_3(\alpha)}{3!}\Phi^{(3)}\left(\alpha_c\right) + \ldots. \tag{7}$$

$$P(\xi_k > \xi_c) = 1 - \int_{-\infty}^{\xi_c} \Phi\left(\xi_c\right) + \frac{c_1(\xi)}{1!}\Phi^{(1)}\left(\xi_c\right) + \frac{c_3(\xi)}{3!}\Phi^{(3)}\left(\xi_c\right) + \ldots. \tag{8}$$

where α_c is the critical margin for damping constant, ξ_c is the critical margin for damping factor, Φ is the cumulative density function of standard normal distribution and c_1, c_2, c_3, c_4 are the coefficients. More details about the theory of cumulants and way to obtain the value of these coefficients can be found in [3–6]. Equations (7) and (8) provide important statistical information about SSS; a higher value of these indices suggest that the system has a high likelihood of being small-signal stable with respect to its margins and vice versa.

4 Design and optimization of PODC parameters

This section first discusses the design of PODC and the procedure to optimize its parameters using different SIOA.

4.1 Modeling of PODC for RES converters

Figure 4 shows the structure of PODC located at ith RES converter in our study. It is a cascade connection of two main

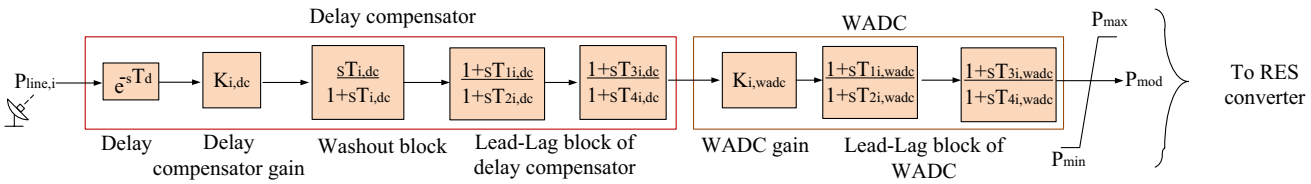

Fig. 4 Structure of PODC located at ith RES farm

controllers: First, the delay compensator which eliminates the phase lag caused due to latency in communication and second the commonly used structure of wide area damping controller (WADC) to enhance SSS [12]. Different electrical variables such as bus voltage, active and reactive power flow, and the angular difference can be taken as a feedback signal for PODCs. However, bus voltage and reactive power flow contains flux decay components, and angular difference requires an additional phase lead of 90° [33]. Therefore, the active power flowing through line i $P_{\text{line},i}$ is taken as input for the PODC and the communication delay to send this signal to POD is modeled as e^{-sT_d} in our work [1]. The best feedback to PODC among many signals is selected using the residue method [20]. The lead–lag time constants for PODC at ith location are: $T_{1i,\text{dc}}, T_{2i,\text{dc}}, T_{3i,\text{dc}}, T_{4i,\text{dc}}$, washout time constant is $T_{i,\text{dc}}$ and gain is $K_{i,\text{dc}}$. The lead time constants for WADC at ith location are: $T_{1i,\text{wadc}}, T_{2i,\text{wadc}}, T_{3i,\text{wadc}}, T_{4i,\text{wadc}}$ and WADC gain is $K_{i,\text{wadc}}$. The output from the damping controller P_{mod} has a maximum $P_{\max}$ and minimum $P_{\min}$ whose values equal to 0.2 p.u., and -0.2 p.u., respectively. More values of other PODC parameters used in our study are given in Sect. 4.2.1. The output from the PODC is chosen to modulate the active power loop of RES converter in our study as the damping performance is independent to RES size when active power regulation is considered [34]. We have used DIGSILENT built-in wind farm model [35] which is similar to type 4 WTG as well as DIGSILENT built-in solar farm model [35] as the models for WTG and PVG in our study. Moreover, we have also used common two-stage model of PSS [32] at selected generators which has a gain of $K_{i,\text{pss}}$, washout block time constant $T_{i,w}$ and lead–lag blocks parameters of $T_{1i,\text{pss}}, T_{2i,\text{pss}}, T_{3i,\text{pss}}, T_{4i,\text{pss}}$.

4.2 Optimization of PODC parameters

4.2.1 Formulation of the optimization problem

The objective function to optimize the PODC parameters is formulated as:

$$\text{maxm.}F = \sum_{i=1}^{p} P(\alpha_k < \alpha_c) + \sum_{i=1}^{p} P(\xi_k > \xi_c) \tag{9}$$

subject to:

$$\begin{aligned}
&0.1 \le K_{i,\text{pss}}, K_{i,\text{wadc}} \le 50\\
&0.1 \le K_{i,\text{dc}} \le 1\\
&0.01 \le T_{1i,\text{pss}}, T_{3i,\text{pss}}, T_{1i,\text{wadc}}, T_{3i,\text{wadc}}, T_{1i,\text{dc}}, T_{3i,\text{dc}} \le 1.5\\
&0.01 \le T_{2i,\text{pss}}, T_{4i,\text{pss}}, T_{2i,\text{wadc}}, T_{4i,\text{wadc}}, T_{2i,\text{dc}}, T_{4i,\text{dc}} \le 0.15
\end{aligned} \tag{10}$$

Equation (9) is a maximization problem, where the objective is to maximize the probability of damping constant and damping factor of p number of eigenvalues to be greater than their margin values. The values for α_c and ξ_c are taken as -0.1 and 0.1, respectively, in this study and may vary depending upon the user requirement. The range of the constraints given in Eq. (10) is taken from [1, 32].

4.2.2 Solving the optimization problem using different SIOA

As MATLAB provides an excellent platform for coding optimization algorithms, all the optimization programs were written in it. Electrical modeling of the test system and calculation of crucial statistical information about SSS were performed using DIGSILENT software. The major difference between SIOA lies in the updating rules which depend on the type of swarm characteristics used. Thus, we have only explained the application of the proposed method to optimize the parameters of PODCs using BA in detail and provided updating rules and a short description for other optimization algorithms as the implementation process is similar.

4.2.2.1 Bat algorithm Bat algorithm is one of the most popular nature-inspired optimization algorithms and is inspired by the behavior of the bats. The flowchart depicting the utilization of BA to optimize PODC parameters is shown in Fig. 5 and is described below:

i. Initialize the maximum frequency $f_{\max}$, minimum frequency $f_{\min}$, pulse rate r_i and the loudness A_i for a total N_{pop} population of bats.
ii. Generate initial position x_i using random numbers where x_i is a vector of decision variables and is given by:

$$\begin{aligned}
x_i = &\big[K_{i,\text{wadc}}, K_{i,\text{dc}}, K_{i,\text{pss}}, T_{1i,\text{wadc}}, T_{1i,\text{dc}}, T_{1i,\text{pss}}, T_{2i,\text{wadc}}, T_{2i,\text{dc}}, T_{2i,\text{pss}}\\
&T_{3i,\text{wadc}}, T_{3i,\text{dc}}, T_{3i,\text{pss}}, T_{4i,\text{wadc}}, T_{4i,\text{dc}}, T_{4i,\text{pss}}\big]
\end{aligned} \tag{11}$$

iii. Evaluate the fitness value using Eq. (9) and find the current best solution x^*. To evaluate this step, the optimization algorithm in MATLAB sends the command signal to DIGSILENT and waits for DIGSILENT to complete its analysis. DIGSILENT then runs the eigenvalue analysis and calculates the statistical information and send the signal to MATLAB to start its analysis. Meanwhile, DIGSILENT waits for the command signal from MATLAB to conduct further analysis. More details on the technique utilized in this paper to interface MATLAB and DIGSILENT can be found in [36].
iv. Move the bats from current t to new position $t+1$ using the following equations:

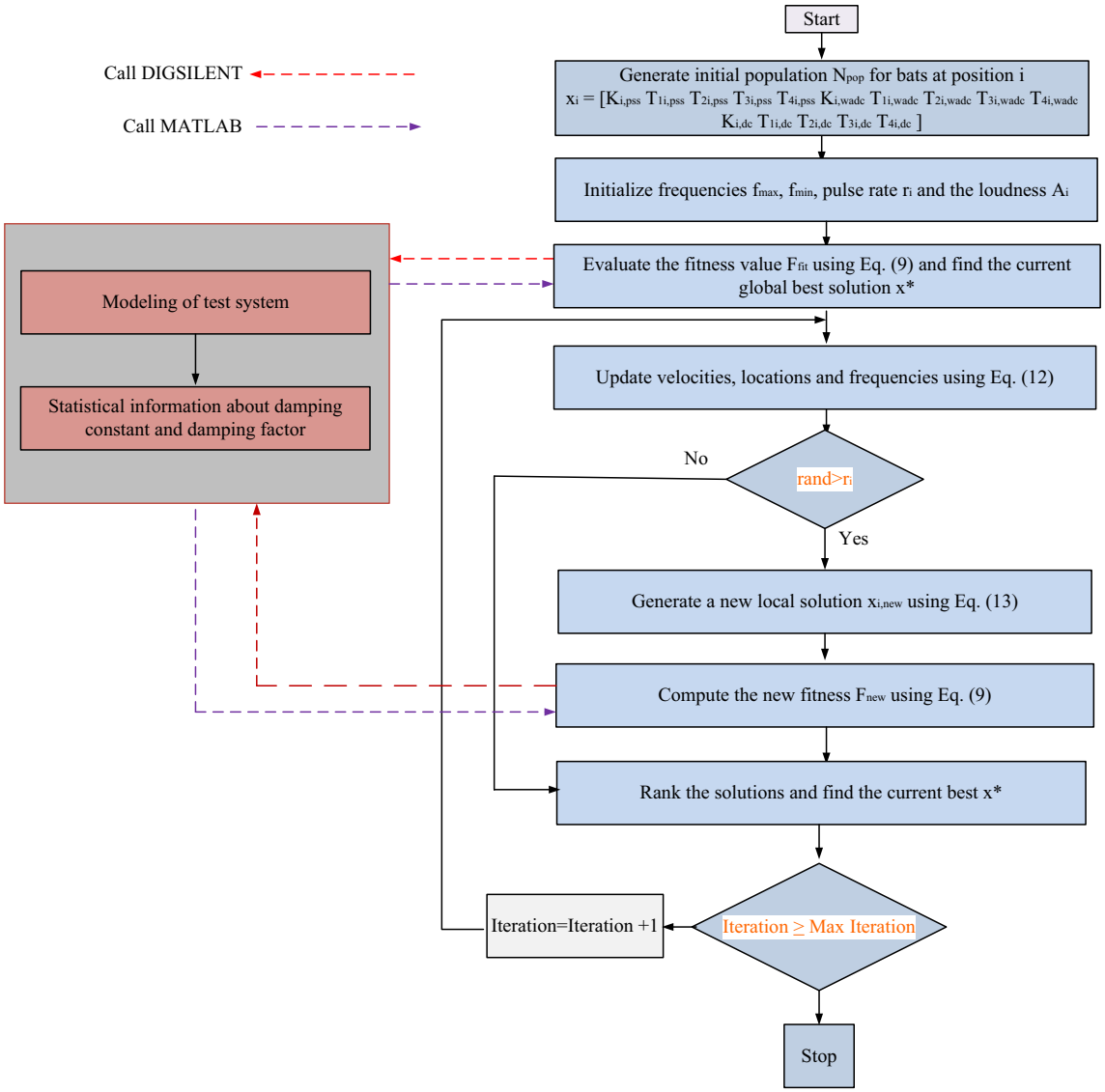

Fig. 5 Flowchart of implementation of the proposed method to tune PODCs in DIGSILENT and MATLAB

$$\begin{aligned} f_i &= f_{\min} + \left(f_{\max} - f_{\min}\right)\beta \\ v_i^{t+1} &= v_i^t + \left(x_i^t - x_*\right)f_i \\ x_i^{t+1} &= x_i^t + v_i^{t+1} \end{aligned} \tag{12}$$

where v_i^{t+1}, v_i^t, x_i^{t+1}, x_i^t, β and x_* are the velocity of bats at $t+1$ location, the velocity of bats at t location, the position of bats at $t+1$ location, the position of bats at t location, a vector of random number, and the current global best solution, respectively.

v. Generate a new solution $x_{i,\text{new}}^{t+1}$ if the random number is greater than r_i using:

$$x_{i,\text{new}}^{t+1} = x_i^{t+1} + \epsilon A^t \tag{13}$$

where ϵ is a random number between -1 and 1. However, if (rand $< r_i$), proceed to step vii.

vi. Calculate the new value of fitness function F_{new} using Eq. (9) and reset the value of the control parameter if it exceeds its range depending upon its nearness to the extreme value using Eq. (10).

vii. Continue to the next iteration until the maximum number of iterations is reached.

4.2.2.2 Firefly algorithm FA is another popular SIOA which is inspired by the flashing characteristics of fireflies. The update rule of FA is given as:

$$x_i^{t+1} = x_i^t + \beta_o e^{-\gamma r_{i,j}^2}\left(x_j^t - x_i^t\right) + \alpha\varepsilon_i^t \tag{14}$$

where $x_i^{t+1}, x_i^t, x_j^t, r_{i,j}, \beta_o, \gamma, \alpha, \varepsilon$ are the locations of x_i fireflies at $t+1$ position, locations of x_i fireflies at t position, locations of x_j fireflies at t position, Cartesian distance between fireflies at i and j position, attractiveness coefficient, coefficient of variation of attractiveness, randomization parameter, and vector of random number, respectively. More details on this algorithm are given in [16, 37].

4.2.2.3 Cuckoo search algorithm The third SIOA we have used in our study is the CSA which is based on the brood parasitism of some cuckoo species. This algorithm uses two updating rules: one local random walk and the other, global random walk. The update rule for the local random walk is given by:

$$x_i^{t+1} = x_i^t + \alpha s \otimes H\left(p_a - \varepsilon\right)\left(x_j^t - x_k^t\right) \tag{15}$$

where $x_i^{t+1}, x_j^t, x_k^t, \alpha, s, H, p_a, \varepsilon$ are the locations of x_i cuckoos at $t+1$ position, random solution j, random solution k, randomization coefficient, step size, Heaviside function and vector of random numbers. The update rule for the global random walk is given by:

$$x_i^{t+1} = x_i^t + \alpha s L(s, \lambda) \tag{16}$$

where λ is the parameter of Levy distribution L. More rigorous details on CSA are given in [37, 38].

4.2.2.4 Particle swarm optimization algorithm The final algorithm we have used in our study is PSO which is the pioneering SIOA. PSO has two updating rules for particle position x_j and particle velocity v_j as follows:

$$\begin{aligned} v_j^{t+1} &= v_j^t + c_1\varepsilon\left(g^* - x_j^t\right) + c_2\beta\left(x_j^* - x_j^t\right) \\ x_j^{t+1} &= x_j^t + v_j^{t+1} \end{aligned} \tag{17}$$

where c_1, c_2 are the weight coefficients and ε, β are the random vectors, respectively.

The detailed description of this algorithm can be found in [36, 37].

5 Results and discussion

5.1 Test system

The test system is a modified 68 bus system which is widely used to study low-frequency oscillatory stability [39] and is shown in Fig. 6. Generators 1 to 12 are assumed to be equipped with PSSs. The modified system has two solar farms, and two wind farms. As the location of RES is not of main concern in our study, we have arbitrarily placed them at the locations as shown in Fig. 7. The rating of both PVG1 and WTG1 is 850 MVA, and the ratings of both PVG2 and WTG2 is 440 MVA which corresponds to the penetration of 20% (aggregate) in their respective areas. This penetration

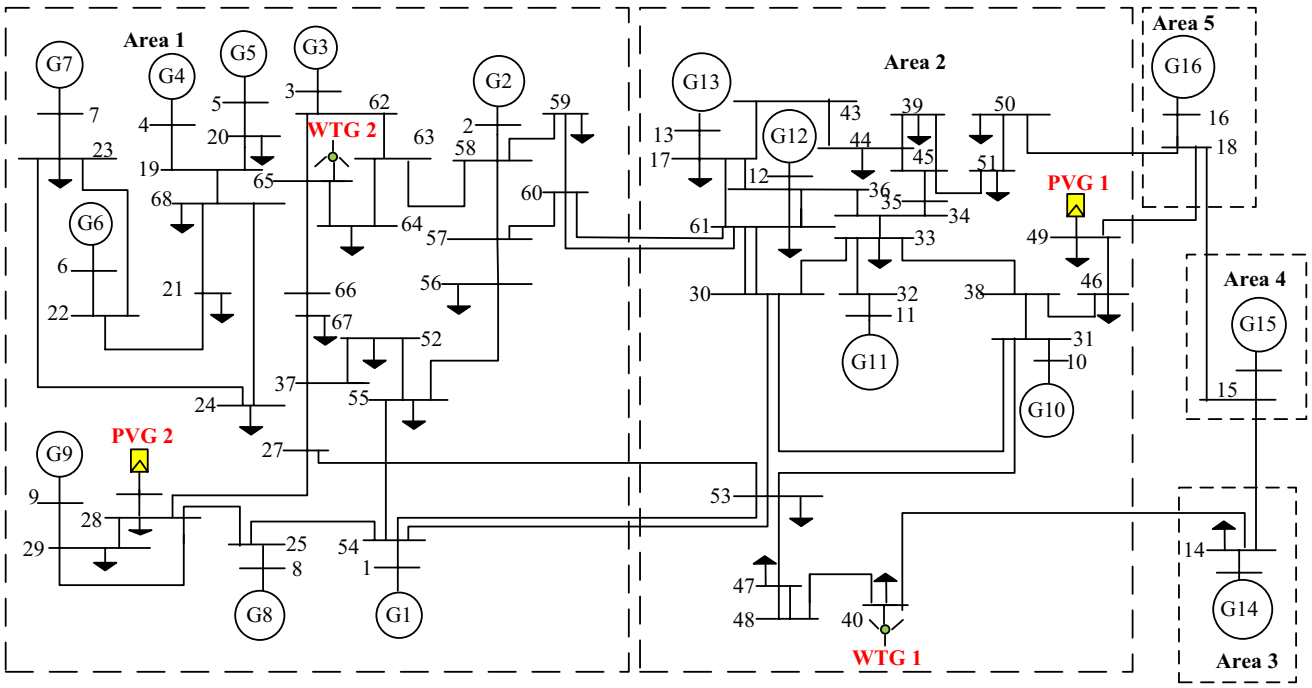

Fig. 6 Modified IEEE 68 bus system with RES

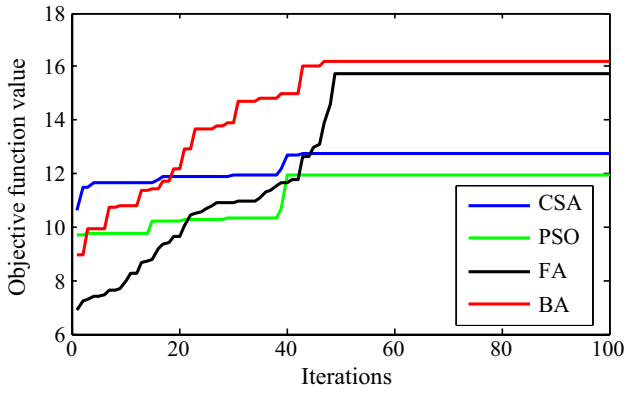

Fig. 7 Convergence of objective function with different SIOA

Table 1 Results from deterministic eigenvalue analysis

Mode number	Damping constant	Damping factor (%)	Frequency (Hz)
1	−0.1435	5.411	0.4216
2	−0.2278	4.675	0.7748
3	−0.0653	1.211	0.8623

level is consistent with the penetration level of many countries which have high variable generation [27]. The details of wind speed characteristics, solar irradiance characteristic, WTG and RES converters used in this paper are taken from [16]. The standard deviation of the load is taken as 10% of the mean value of the load. The details about synchronous generators, line parameters, and load values used in our study are given in [33].

5.1.1 Simulation results

As discussed in Sect. 3, it is first necessary to find the best input feedback signal for each PODC before attempting to tune them. Table 1 shows there are three critical modes (eigenvalues) obtained using deterministic eigenvalue analysis [33] when only PSSs (no PODCs) are present. The PSSs were tuned using the proposed method but discarding the time delay uncertainty. The critical modes are defined as the eigenvalues which have damping constant greater than −0.5, and damping factor less than 10% [9] throughout our study.

Table 3 Comparison of statistical results with four SIOA

	BA	FA	CSA	PSO
Maximum	16.1656	15.7505	12.7270	11.9287
Minimum	8.9368	6.8689	10.6386	9.6925
Average	14.6673	13.0619	12.3552	11.2200
Computation time (h)	5.6990	5.6111	8.2022	5.7554
Number of runs	30	30	30	30

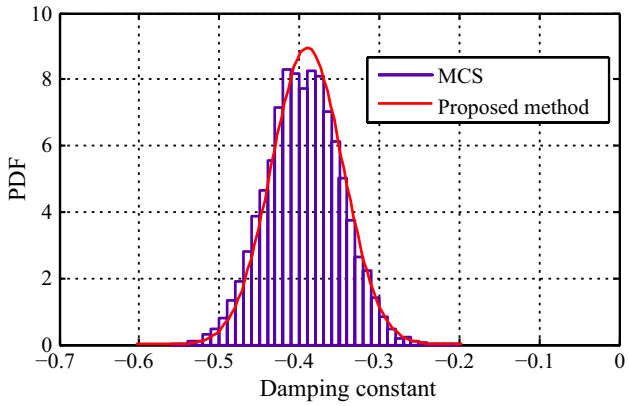

Fig. 8 Comparison of PDFs of damping constant

Table 2 shows the results obtained after using residue analysis [33] to select the best feedback and most suitable PODC for each critical mode. Thus, from Table 2, the best feedback signal for PODC 1, 2, 3 and 4 were found to be active power flowing through line 41 and 42, active power flowing through line 40 and active power flowing through line 41 and 42, and active power flowing through line 45 and 51 respectively. Note that PODC1, PODC2, PODC3, and PODC4 refer to PODC located at PVG1, WTG1, PVG2, and WTG2, respectively.

Once the best feedback signal was found for each PODC, four SIOAs were used to solve the proposed method and the important results obtained are provided in Table 3. All the optimization algorithms were solved using Intel (R) Core (TM) i5-2400 CPU, 3.1 GHz processing speed with 16 GB RAM. A standard population size of 40 and a maximum number of generations of 100 was taken for all optimization algorithms. The parameters for BA, PSO, FA, and CSA are taken from [16, 36, 38, 40], respectively, and are also given

Table 2 Results from residue analysis

Mode 1			Mode 2			Mode 3		
Line	PODC	Residue	Line	PODC	Residue	Line	PODC	Residue
40–41	2	0.1736	41–42	3	0.3483	41–42	1	0.1171
18–50	2	0.1714	30–53	3	0.3394	18–42	1	0.0985
45–51	4	0.1654	17–36	3	0.2824	30–53	3	0.0608

in Table 7 in "Appendix" for convenience. Table 3 shows that the BA provides the highest average value of objective function compared to other optimization algorithm, and thus the result obtained by it was used to optimize the parameters of PODCs.

Furthermore, the value of the objective function with BA also converges to the maximum value compared to other optimization algorithms as shown in Fig. 7 further validating the choice of BA. The optimization algorithm requires calculation of the fitness value of the objective function. This value is calculated using the probabilistic assessment method described in Sect. 3 of the manuscript, and the average computation time for it is around 5 s. Thus, while running the optimization algorithm, a delay of 5 s is added for each population. Furthermore, we have used 100 generations for the optimization problem causing the overall computational time to be around 5 h.

As the proposed method is based on the probabilistic approach, it was first verified with Monte Carlo simulation (MCS), and the plot of PDFs of damping constant of mode

Table 4 Comparison of stability indices under different controller conditions and different scenarios

Scenario	Mode number	Controller design	Damping factor			Damping constant		
			$\bar{\alpha}$	σ_α	$P(\alpha < -0.1)$ (%)	$\bar{\xi}$	σ_ξ	$P(\xi > 0.1)$ (%)
1	1	No PODCs	−0.0696	0.0452	25.0800	0.0129	0.0001	0
1	1	RM	−0.2844	0.0454	100	0.1114	0.0040	99.7800
1	1	OBTM	−0.6934	0.0453	100	0.1228	0.0025	100
1	1	Proposed method	−0.6915	0.0466	100	0.1719	0.0110	**100**
1	2	No PODCs	−0.1294	0.0452	74.2200	0.0490	0.0008	0
1	2	RM	−0.1464	0.0454	84.0100	0.0623	0.0041	0
1	2	OBTM	−0.2446	0.0453	99.9300	0.1013	0.0025	69.0400
1	2	Proposed method	−0.3938	0.0466	100	0.1872	0.0109	**100**
1	3	No PODCs	−0.1862	0.0452	97.1700	0.0509	0.0005	0
1	3	RM	−0.1416	0.0454	82.0100	0.0408	0.0041	0
1	3	OBTM	−0.2346	0.0453	99.8500	0.0544	0.0025	0
1	3	Proposed method	−0.6813	0.0466	100	0.1387	0.0108	**99.98**
2	1	No PODCs	−0.0773	0.0452	30.8000	0.0141	0.0001	0
2	1	RM	−0.9382	0.0454	100	0.1630	0.0015	100
2	1	OBTM	−0.7281	0.0456	100	0.1266	0.0058	100
2	1	Proposed method	−0.6923	0.0457	100	0.1427	0.0059	**100**
2	2	No PODCs	−0.1258	0.0452	71.6100	0.0141	0.0001	0
2	2	RM	−0.1820	0.0452	100	0.2042	0.0059	100
2	2	OBTM	−0.2739	0.0456	99.9900	0.0635	0.0058	0
2	2	Proposed method	−0.4438	0.0456	100	0.2042	0.0059	**100**
2	3	No PODCs	−0.1736	0.0453	94.8000	0.0465	0.0002	0
2	3	RM	−0.1499	0.0453	86.4800	0.0430	0.0015	0
2	3	OBTM	−0.2493	0.0457	99.95	0.1087	0.0058	93.5200
2	3	Proposed method	−0.4883	0.0459	100	0.1430	0.0062	**100**
3	1	No PODCs	−0.0773	0.0452	30.8000	0.0141	0.0087	0
3	1	RM	−0.2581	0.0452	99.9800	0.0823	0.0008	0
3	1	OBTM	−0.6562	0.0455	100	0.1820	0.0018	100
3	1	Proposed method	−0.4438	0.0452	100	0.2042	0.0009	**100**
3	2	No PODCs	−0.2195	0.0461	99.5200	0.0562	0.0088	0
3	2	RM	−0.2471	0.0454	99.9400	0.1119	0.0003	100
3	2	OBTM	−0.5185	0.0464	100	0.1109	0.0031	99.9800
3	2	Proposed method	−0.7513	0.0455	100	0.1830	0.0019	**100**
3	3	No PODCs	−0.1407	0.0460	81.1700	0.0274	0.0087	0
3	3	RM	−0.3944	0.0453	100	0.0823	0.0008	0
3	3	OBTM	−0.6034	0.0457	100	0.1118	0.0019	100
3	3	Proposed method	−0.6923	0.0453	100	0.1427	0.0008	**100**

Table 5 Details of different scenarios

No.	Details
1	Normal loading condition
2	Increase the load of the whole system by 5%
3	Decrease the load of the whole system by 2%

1 obtained using two methods is shown in Fig. 8. It can be clearly seen that the two plots are very similar highlighting the accuracy of the proposed method.

Table 4 shows the different statistical results such as shows the different statistical results such as mean $\bar{\alpha}$ and standard deviation of damping constant σ_α of critical modes, mean $\bar{\xi}$ and standard deviation of damping factor σ_ξ of critical modes, as well as the likelihood of stability with respect to their margins for different controller configurations as well for different scenarios (Table 5). All of these probabilistic stability indices are calculated using the assessment method described in Sect. 3. It was found that when the system loads were increased by more than 5% of their original value and decreased by less than 2% of their original value, the load flow analysis failed to converge. Hence, we have chosen those two conditions to define as scenarios 2 and 3 as given in Table 5. We have also compared the results obtained using the proposed method with two other methods: one conventional technique based on residue method (RM) [13] and other optimization-based tuning method (OBTM) [18] in our study.

Table 4 shows that there are three critical modes under scenario 1. These modes have a very high likelihood that their damping factor is less than the desired damping factor, as well as damping constant, is greater than the critical damping constant when no PODCs are used. However, the value of the probabilistic stability indices improves with RM and OBTM and are highest with the PODCs tuned using the proposed method. Furthermore, similar conclusions can also be made for the analysis conducted for scenarios 2 and 3. These results show that the PODCs tuned using the proposed method are highly robust against stochastic time delay and other power system uncertainties and is highly effective

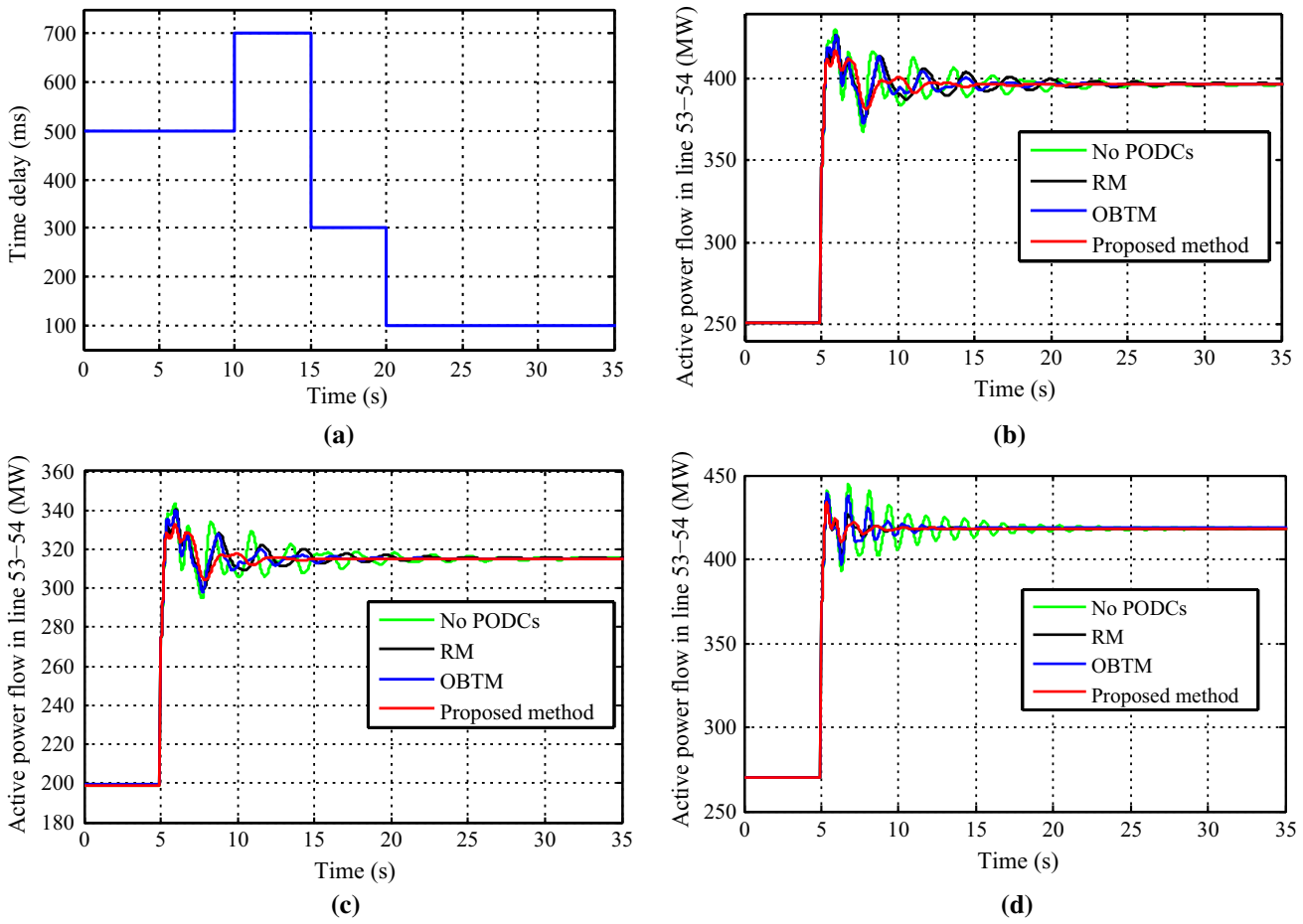

Fig. 9 Time responses of power in line 53–54 under varying time delay. **a** Input model of varying time delay, **b** responses for different controllers under scenario 1, **c** responses of different controllers under scenario 2, **d** responses of different controllers under scenario 3

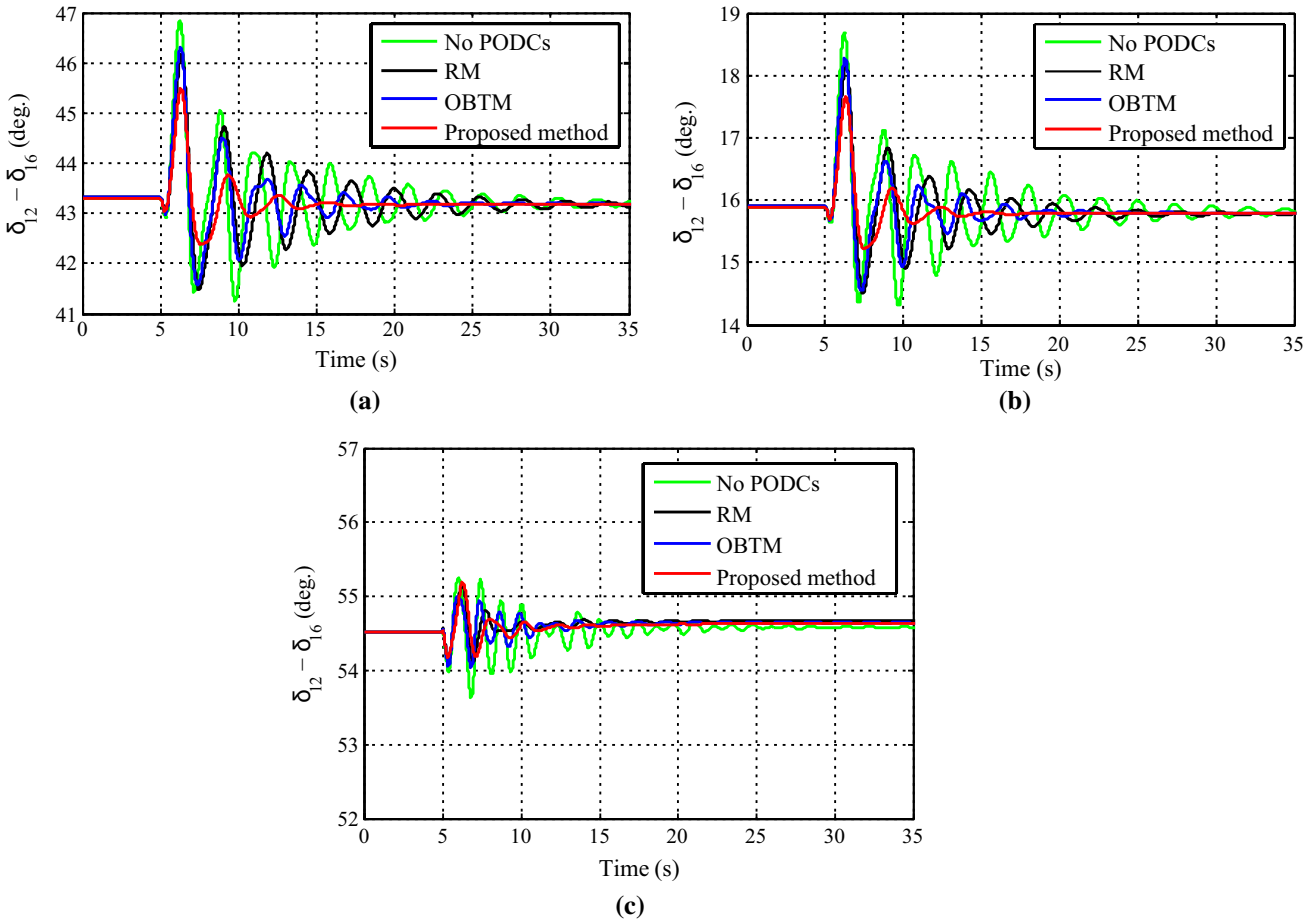

Fig. 10 Time responses of δ_{12-16} under varying time delay. **a** Responses for different controllers under scenario 1, **b** responses for different controllers under scenario 2, **c** responses for different controllers under scenario 3

in improving SSS. The result obtained with the proposed method is shown in bold color in Table 4.

In addition, we have also conducted extensive time domain simulations (TDS) to show the effectiveness of the PODCs tuned using the proposed method under variable time delay. We have chosen active power flowing through one of the circuits of the critical line (line connecting bus 53 and 54) as the variable of interest for the TDS. The model of varying input delay used for our TDS is shown in Fig. 9a which sufficiently covers the real-world time delay in WAMS stated in Sect. 4.1. Figure 9b, c, d, shows the time responses of the critical line when one of its circuits is removed at 5 s following a three-phase line to ground fault. It can be clearly seen that the time responses with the proposed method are much superior to other methods further validating the effectiveness of the proposed method.

Figure 10 shows the result of TDS for the relative rotor angle of one of the largest generators, Gen. 12 δ_{12} with respect to the rotor angle of the reference machine, Gen. 16 δ_{16}. Both Fig. 10 and Table 6 show that the overshoot (*OS*) and settling time (T_s) of time responses with the PODCs parameter optimized using the proposed method is much lower compared to other methods. This further highlights the effectiveness of the ability of PODCs tuned using the proposed method to successfully damp the power oscillations under varying time delay compared to existing methods.

Table 6 Comparison of time responses of δ_{12-16} under different methods and scenarios

Scenario	No PODCs		RM		OBTM		Proposed method	
	OS (%)	T_s (s)	*OS* (%)	T_s (s)	*OS* (%)	T_s (s)	*OS* (%)	T_s (s)
1	8.3837	34.3867	6.9786	32.6333	7.2408	20.9010	5.3478	12.5110
2	18.2152	34.4577	15.2465	26.4314	15.7249	20.5887	10.8406	12.0630
3	1.2140	30.8704	0.8848	23.4614	0.6599	28.6733	0.9250	11.5752

6 Conclusion

This paper utilizes the proposed method based on a probabilistic approach to optimize the parameters of PODC incorporated in RES converters to enhance the system SSS considering variable time and other important power system uncertainties. Our study has identified the following findings:

i. The proposed method can accurately assess the effect of different power system uncertainties on system SSS.
ii The minimum low-frequency oscillatory margin with respect to the damping factor with the PODC tuned using the OBTM is 0% for scenarios 1 and 2, and 99.9800% for scenario 3, whereas the minimum SSS margin with respect to the damping factor with the PODCs designed using the RM is 0% for all the scenarios. The value of this quantity is always higher than 99.9800% for the PODCs designed using the proposed method.
iii. The maximum value of OS and T_s when the PODCs are designed using the proposed method are 10.8406% and 12.5110 s, respectively, which are lower than the values obtained after utilization of the controllers designed using the compared methods.
iv. BA provides the best result (Average = 14.6673) compared to FA (Average = 13.0619), CSA (Average = 12.3552), PSO (Average = 11.2200) for our study.

Our future studies will try to reduce the computational time of the proposed method by using mathematical optimization techniques.

Acknowledgements The authors would like to express thanks for the Petchra-Pra Jom Klao research scholarship, funded by the King Mongkut's University of Technology Thonburi for the support.

Appendix

Optimization algorithm parameters

See Table 7.

Table 7 Parameters of different SIOA

Population size	Maximum iterations	BA			FA		PSO			CSA		
		f_{max}	f_{min}	α	β	γ	α	c_1	c_2	p_a	s	α
40	100	2	0	0.2	0.1	1	0.2	0.6	0.3	0.5	0.005	0.2

References

1. Yao W, Jiang L, Wen J, Wu Q, Cheng S (2014) Wide-area damping controller of facts devices for inter-area oscillations considering communication time delays. IEEE Trans Power Syst 29(1):318–329
2. Hasan KN, Preece R (2018) Influence of stochastic dependence on small disturbance stability and ranking uncertainties. IEEE Trans Power Syst 33(3):3227–3235
3. Bu S, Du W, Wang H, Chen Z, Xiao L, Li H (2012) Probabilistic analysis of small-signal stability of large-scale power systems as affected by penetration of wind generation. IEEE Trans Power Syst 27(2):762–770
4. Bu S, Du W, Wang H (2013) Probabilistic analysis of small-signal rotor angle/voltage stability of large-scale AC/DC power systems as affected by grid connected offshore wind generation. IEEE Trans Power Syst 28(4):3712–3719
5. Bu S, Du W, Wang H (2015) Investigation on probabilistic small-signal stability of power systems as affected by offshore wind generation. IEEE Trans Power Syst 30(5):2479–2486
6. Gurung S, Naetiladdanon S, Sangswang A (2019) Probabilistic small-signal stability analysis of power system with solar farm integration. Turk J Electr Eng Comput Sci 27(2):1276–1289
7. Rueda JL, Colomé DG, Erlich I (2009) Assessment and enhancement of small signal stability considering uncertainties. IEEE Trans Power Syst 24(1):198–207
8. Bian X, Geng Y, Lo KL, Fu Y, Zhou Q (2016) Coordination of PSSs and SVC damping controller to improve probabilistic small-signal stability of power system with wind farm integration. IEEE Trans Power Syst 31(3):2371–2382
9. Huang H, Chung C (2012) Coordinated damping control design for DFIG-based wind generation considering power output variation. IEEE Trans Power Syst 27(4):1916–1925
10. Mokhtari M, Aminifar F (2014) Toward wide-area oscillation control through doubly-fed induction generator wind farms. IEEE Trans Power Syst 29(6):2985–2992
11. Shah R, Mithulananthan N, Lee KY et al (2013) Large-scale PV plant with a robust controller considering power oscillation damping. IEEE Trans Energy Convers 28(1):106–116
12. Surinkaew T, Ngamroo I (2019) Inter-area oscillation damping control design considering impact of variable latencies. IEEE Trans Power Syst 34(1):481–493
13. He J, Lu C, Wu X, Li P, Wu J (2009) Design and experiment of wide area HVDC supplementary damping controller considering time delay in China southern power grid. IET Gener Transm Distrib 3(1):17–25
14. Preece R, Milanović JV (2014) Tuning of a damping controller for multiterminal VSC-HVDC grids using the probabilistic collocation method. IEEE Trans Power Deliv 29(1):318–326
15. Yongli Z, Chengxi L, Bin W, Kai S (2018) Damping control for a target oscillation mode using battery energy storage. J Mod Power Syst Clean Energy 6(4):833–845
16. Gurung S, Naetiladdanon S, Sangswang A (2019) Coordination of power system stabilizers and battery energy-storage system controllers to improve probabilistic small-signal stability considering integration of renewable-energy resources. Appl Sci 9(6):1109. https://doi.org/10.3390/app9061109
17. Cai G, Yang D, Liu C (2013) Adaptive wide-area damping control scheme for smart grids with consideration of signal time delay. Energies 6(9):4841–4858
18. Shakarami M, Davoudkhani IF (2016) Wide-area power system stabilizer design based on grey wolf optimization algorithm considering the time delay. Electr Power Syst Res 133:149–159

19. Beiraghi M, Ranjbar A (2016) Adaptive delay compensator for the robust wide-area damping controller design. IEEE Trans Power Syst 31(6):4966–4976
20. Cheng L, Chen G, Gao W, Zhang F, Li G (2014) Adaptive time delay compensator (ATDC) design for wide-area power system stabilizer. IEEE Trans Smart Grid 5(6):2957–2966
21. Liu M, Dassios I, Tzounas G, Milano F (2019) Stability analysis of power systems with inclusion of realistic-modeling WAMS delays. IEEE Trans Power Syst 34(1):627–636
22. Duan J, Xu H, Liu W (2018) Q-learning-based damping control of wide-area power systems under cyber uncertainties. IEEE Trans Smart Grid 9(6):6408–6418
23. Mokhtari M, Aminifar F, Nazarpour D, Golshannavaz S (2013) Wide-area power oscillation damping with a fuzzy controller compensating the continuous communication delays. IEEE Trans Power Syst 28(2):1997–2005
24. Zhou J, Ke D, Chung C, Sun Y (2018) A computationally efficient method to design probabilistically robust wide-area PSSs for damping inter-area oscillations in wind-integrated power systems. IEEE Trans Power Syst 33(5):5692–5703
25. Wang Z, Chung C, Wong K, Tse C (2008) Robust power system stabiliser design under multi-operating conditions using differential evolution. IET Gener Transm Distrib 2(5):690–700
26. Zhang X, Lu C, Xie X, Dong ZY (2016) Stability analysis and controller design of a wide-area time-delay system based on the expectation model method. IEEE Trans Smart Grid 7(1):520–529
27. REN21 R (2018) Global Status Report, REN21 Secretariat, Paris, France. Tech. Rep
28. Preece R, Huang K, Milanović JV (2014) Probabilistic small-disturbance stability assessment of uncertain power systems using efficient estimation methods. IEEE Trans Power Syst 29(5):2509–2517
29. Naduvathuparambil B, Valenti MC, Feliachi A (2002) Communication delays in wide area measurement systems. In: Proceedings of the thirty-fourth southeastern symposium on system theory (Cat. No. 02EX540). IEEE, pp 118–122
30. Stahlhut JW, Browne TJ, Heydt GT, Vittal V (2008) Latency viewed as a stochastic process and its impact on wide area power system control signals. IEEE Trans Power Syst 23(1):84–91
31. Lu C, Zhang X, Wang X, Han Y (2015) Mathematical expectation modeling of wide-area controlled power systems with stochastic time delay. IEEE Trans Smart Grid 6(3):1511–1519
32. Sauer PW, Pai M (1998) Power system dynamics and stability, vol 1. Prentice Hall, London
33. Pal B, Chaudhuri B (2006) Robust control in power systems. Springer, Berlin
34. Ruan SY, Li GJ, Ooi BT, Sun YZ (2008) Power system damping from real and reactive power modulations of voltage-source-converter station. IET Gener Transm Distrib 2(3):311–320
35. DIgSILENT Gmbh (2018) User Manual. http://www.digsilent.de/en/downloads.html. Accessed 1 Mar 2019
36. Stativa A, Gavrilaş M, Stahie V (2012) Optimal tuning and placement of power system stabilizer using particle swarm optimization algorithm. In: 2012 International conference and exposition on electrical and power engineering. IEEE, pp 242–247
37. Yang XS (2014) Cuckoo search and firefly algorithm: overview and analysis. In: Cuckoo search and firefly algorithm. Springer, Berlin, pp 1–26
38. Elazim SA, Ali E (2016) Optimal power system stabilizers design via cuckoo search algorithm. Int J Electr Power Energy Syst 75:99–107
39. Canizares C, Fernandes T, Geraldi E, Gerin-Lajoie L, Gibbard M, Hiskens I, Kersulis J, Kuiava R, Lima L, DeMarco F et al (2017) Benchmark models for the analysis and control of small-signal oscillatory dynamics in power systems. IEEE Trans Power Syst 32(1):715–722
40. Sambariya D, Prasad R (2014) Robust tuning of power system stabilizer for small signal stability enhancement using metaheuristic bat algorithm. Int J Electr Power Energy Syst 61:229–238